

Reply to "Comment on 'Exactly central heavy-ion collisions by nuclear hydrodynamics'"

H. H. K. Tang

Center for Theoretical Physics, Massachusetts Institute of Technology, Cambridge, Massachusetts 02139

Cheuk-Yin Wong

Physics Division, Oak Ridge National Laboratory, Oak Ridge, Tennessee 37830

We reply to a recent comment concerning our work on nuclear hydrodynamics. A previous numerical error is corrected, and a sample of corrected results is presented.

[NUCLEAR REACTIONS Heavy-ion reactions, nuclear hydrodynamics.]

With regard to the questions raised in a recent communication¹ concerning our paper,² we have found a numerical error in the program. The error originates from an erroneous time scale (by a factor of 1/2) in the propagation along the axis of symmetry. The result of this is that the colliding nuclei move slower than they should according to the bombarding energies cited.

The correct density plots and angular distributions are now presented for the reactions $^{20}\text{Ne} + ^{197}\text{Au}$ at bombarding energies of 100 MeV per nucleon. In Figs. 1 and 2 we give the density contours in the collision of ^{20}Ne on ^{197}Au at 100 MeV per projectile (^{20}Ne) nucleon. The density

contour is graded every 0.025 nucleon/ fm^3 . One observes the main features in the formation of the shock region and the emission of particles with a sidesplash for a small projectile on a heavy target. Figure 1 is for the case of $\eta = \zeta = 10^{-4}$ MeV/ fm^2c , and $\kappa = 10^{-4}$ c/ fm^2 which for simplicity will be called the case of small transport coefficients, and Fig. 2 for $\eta = 0.75$ MeV/ fm^2c , $\zeta = 18.76$ MeV/ fm^2c , and $\kappa = 0.014$ c/ fm^2 which we call the case of large transport coefficients. As one observes, the maximum density reached is higher for the case with small transport coefficients, as compared to the case with large transport coef-

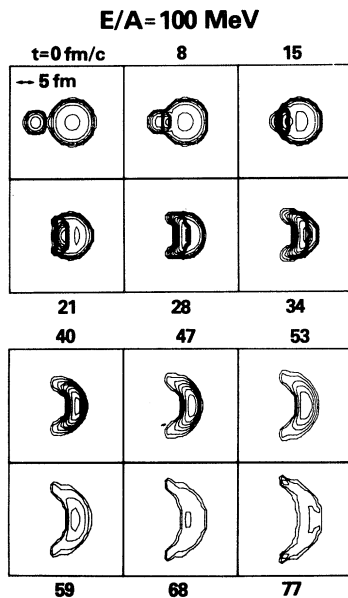


Fig. 1. Evolution of the density field for $^{20}\text{Ne} + ^{197}\text{Au}$ at 100 MeV per projectile (^{20}Ne) nucleon given in the center-of-mass system. The density contours are graded every 0.025 nucleon/ fm^3 . The set of small transport coefficients ($\eta = \zeta = 10^{-4}$ MeV/ fm^2c , and $\kappa = 10^{-4}$ c/ fm^2) are used.

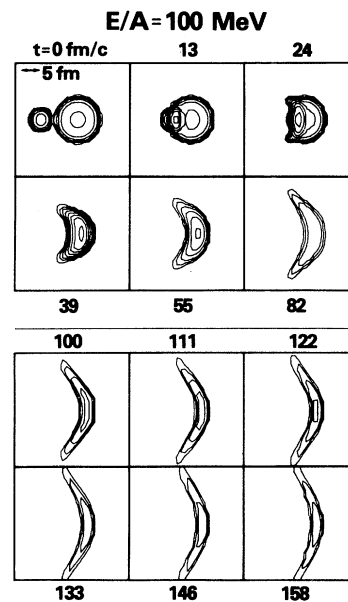


Fig. 2. Evolution of the density field for $^{20}\text{Ne} + ^{197}\text{Au}$ at 200 MeV per projectile (^{20}Ne) nucleon given in the center-of-mass system. The density contours are graded every 0.025 nucleon/ fm^3 . The set of large transport coefficients ($\eta = 0.75$ MeV/ fm^2c , $\zeta = 18.76$ MeV/ fm^2c , and $\kappa = 0.014$ c/ fm^2) are used.

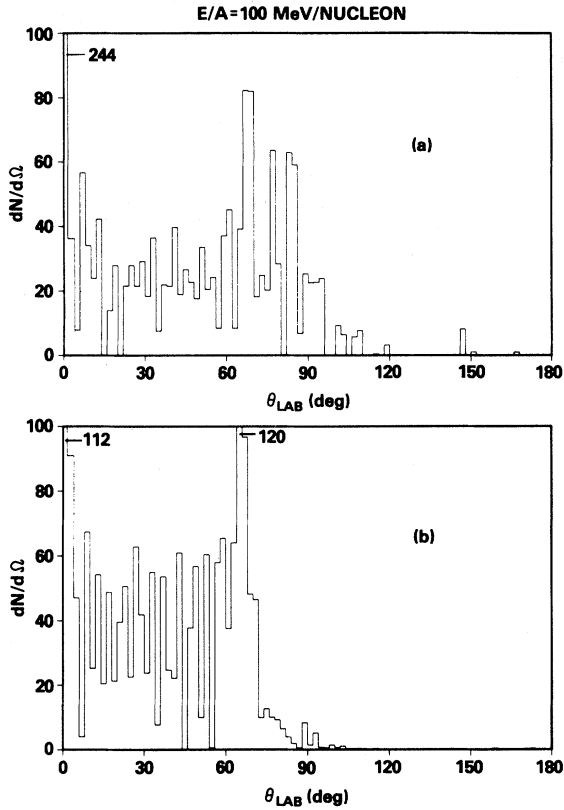


FIG. 3. Laboratory angular distribution $dN/d\Omega$ for the $^{20}\text{Ne} + ^{197}\text{Au}$ reaction at 100 MeV per projectile (^{20}Ne) nucleon. Figure (3a) is for the case of small transport coefficients and (3b) for the case of large transport coefficients.

icients. The density contour is also smoother for the latter case. The side-splash angle is different for the two cases, leading to a difference in the angular distribution. Figure 3a gives the angular distribution for small transport coefficients, while 3b for large transport coefficients. There are more emitted particles in the $80^\circ - 100^\circ$ range in the case of small transport coefficients as compared with the case of large transport coefficients. The energy distributions for the two cases are summarized in Table I. The average energy of emitted particle is 5.66 MeV in the laboratory system for the case with small transport coefficients and is 4.17 MeV for the case with large transport coefficients. Similar differences in density contours, angular distributions and energy distributions can be observed in the higher energy results. One observes that as energy increases, the particles come out more and more towards the back angles. On the other hand, small transport coefficients always lead to a sidesplash at a larger backward angle, as compared with the case of large transport coefficients. Also, the average kinetic energy of the emitted nucleon increases as the bombarding energy increases. The kinetic energy is also greater for the case of small transport coefficients as compared with the case for large transport coefficients.

Reference 1 also raised a number of questions concerning the sizes of the viscosity coefficients. It should be pointed out that the validity of the hydrodynamical description for heavy-ion collisions is still a subject of current investigation. Without a rigorous theoretical resolution of this question, the estimates of the viscosity coefficients for a finite nucleus are model-dependent and are subject to re-

TABLE I. The angular distribution, mean energy, and energy width for collision $^{20}\text{Ne} + ^{197}\text{Au}$ at an energy of 100 MeV per nucleon. Table I(a) is for the case $\eta = \zeta = 10^{-4}$ MeV/($\text{fm}^2 c$) and $\kappa = 10^{-4}$ c/fm^2 and Table I(b) for $\eta = 0.75$ MeV/($\text{fm}^2 c$), $\zeta = 18.76$ MeV/($\text{fm}^2 c$), and $\kappa = 0.014$ c/fm^2 . The quantity \bar{E} is the average energy within the angular bin and σ_E is the $\sqrt{\langle(E-E)^2\rangle}$ within the bin.

θ_{lab} (deg)	(a) Small transport coefficients			(b) Large transport coefficients		
	$dN/d\Omega$ (nucleon/sr)	\bar{E} (MeV)	σ_E (MeV)	$dN/d\Omega$ (nucleon/sr)	\bar{E} (MeV)	σ_E (MeV)
0-20	26.6	2.90	2.10	37.6	2.37	1.50
20-40	20.9	2.69	1.51	37.3	2.31	1.06
40-60	24.6	4.55	3.67	37.5	3.05	1.76
60-80	40.9	8.08	4.50	44.3	5.45	3.06
80-100	22.2	4.93	3.75	3.04	11.9	9.41
100-120	3.33	2.11	0.68	0.339	11.3	7.16
120-140	0	0	0	0.093	3.4	1.91
140-160	0.998	2.0	0	0.145	2.0	0
160-180	0.129	26.0	0	0.076	2.0	0
0-180		5.66			4.17	

visions as more information becomes available.

The research was sponsored by the Division of Basic Energy Sciences, U. S.

Department of Energy, under contract W-7405-eng-26 with the Union Carbide Corporation.

¹L. P. Csernai and H. Stöcker, Phys. Rev. C (in press).

²H. K. Tang and C. Y. Wong, Phys. Rev. C 21, 1846 (1980).